HHS Public Access

Author manuscript

Immunohorizons. Author manuscript; available in PMC 2019 June 25.

Published in final edited form as:

Immunohorizons. 2019 March ; 3(3): 110–120. doi:10.4049/immunohorizons.1900001.

Central Roles of OX40L-OX40 Interaction in the Induction and Progression of Human T Cell-Driven Acute Graft-versus-Host Disease

Trivendra Tripathi[*,†,1], **Wenjie Yin**[†,1], **Yaming Xue**[†], **Sandra Zurawski**[†], **Haruyuki Fujita**[†], **Shino Hanabuchi**[†], **Yong-Jun Liu**[‡,†], **SangKon Oh**[*,†], and **HyeMee Joo**[*,†]

[*]Department of Immunology, Mayo Clinic, Scottsdale, AZ 85259

[†]Baylor Institute for Immunology Research, Dallas, TX 75204

[‡]Sanofi R&D, Cambridge, MA 01701

Abstract

Graft-versus-host disease (GVHD) is one of the major obstacles for the success of allogeneic hematopoietic stem cell transplantation. Here, we report that the interaction between OX40L and OX40 is of critical importance for both induction and progression of acute GVHD (aGVHD) driven by human T cells. Anti-human OX40L monoclonal antibody (hOX40L) treatment could thus effectively reduce the disease severity in a xenogeneic-aGVHD (x-aGVHD) model in both preventative and therapeutic modes. Mechanistically, blocking OX40L-OX40 interaction with an anti-hOX40L antibody reduces infiltration of human T cells in target organs, including liver, gut, lung, and skin. It also decreases IL-21- and TNF-producing T cell responses, while promoting regulatory T cell (Treg) responses without compromising the cytolytic activity of $CD8^+$ T cells. Single blockade of hOX40L was thus more effective than dual blockade of IL-21 and TNF in reducing the severity of aGVHD as well as mortality. Data from this study indicate that OX40L-OX40 interactions play a central role in the pathogenesis of aGVHD induced by human T cells. Therapeutic strategies that can efficiently interrupt OX40L-OX40 interaction in patients might have potential to provide patients with an improved clinical benefit.

Introduction

Allogeneic hematopoietic stem cell transplantation (HSCT) offers great opportunities for curing hematologic malignancies. However, graft-versus-host disease (GVHD) is one of the major causes of HSCT failure. Current post-transplant prophylaxis is primarily based on the use of non-specific immunosuppressive drugs, which include corticosteroids, calcineurin inhibitors, methotrexate, mycophenolate mofetil, and sirolimus (1–4). Such non-specific immunosuppression neither spares pre-existing memory cells nor discriminates between

Correspondence: HyeMee Joo, Department of Immunology, Mayo Clinic, 13400 E Shea Blvd. Scottsdale, AZ 85259, joo.hyemee@mayo.edu.

[1]T.T. and W.Y. contributed equally to this study.

Disclosures

S. Z., H. F., S. H., Y-J. L., S. O., and H. J. are listed as inventors on patent applications concerning the anti-hOX40L monoclonal antibody; the rest of the authors have declared that no conflict of interest exists.

alloreactive and non-alloreactive T cells. Thus, controlling GVHD with non-specific immunosuppressive drugs comes at the cost of increased graft failure, disease relapse, drug toxicity, and compromised immunity to post-transplant infections, such as cytomegalovirus (5). Even though glucocorticoid treatment is a first-line therapy, a substantial number of patients are not responsive to it (6), and the management of steroid refractory acute GVHD (aGVHD), which is associated with poor prognosis, often requires custom-tailored therapy due to the lack of standardized preventive measures. Therefore, it is important to develop a new strategy that can prevent and treat aGVHD while preserving host immunity to infections and graft-versus-leukemia (GVL) effect.

Dendritic cells (DCs) play an important role in the development of aGVHD after transplantation (7–9). Accordingly, depletion of DCs or blockades of certain costimulatory molecules result in improved allograft survivals with a reduced incidence of GVHD (7, 8, 10). Among the costimulatory molecules, OX40L is known to contribute to T cell-driven inflammatory diseases, including asthma, experimental autoimmune encephalomyelitis, collagen-induced arthritis, and fibrosis (11–15). Previous studies have also shown that blocking OX40L early in the post-bone marrow transplantation (BMT) period reduces the severity of aGVHD manifestations in murine and non-human primates (16–18). Such preventative effect of OX40L blockade is independent of signal transducer and activator of transcription (STAT)-4 for T helper 1 (Th1) or STAT-6 for Th2 signaling (17). In addition, another study also reported that anti-mouse OX40L antibody treatment reduces aGVHD manifestations in BMT, but with an increase of Th2 responses (19). In contrast to the data generated in animals (16, 19), OX40L expressed on human DCs is well known to play a key role in the induction and promotion of inflammatory Th2 responses with an increase of STAT-6 activation (20–22). Recently, we and others have also demonstrated a pivotal role of OX40L in promoting T follicular helper (Tfh) cell responses (23, 24). It is thus important to test whether OX40L-OX40 interaction is also a critical component for the induction and progression of aGVHD induced by human antigen presenting cells (APCs) and T cells. Furthermore, understanding the mechanisms by which OX40L blockade ameliorates aGVHD manifestations induced by human immune cells will also be fundamental for the clinical development of OX40L blockade in future. In this study, we thus investigated whether OX40L-OX40 interaction is a critical component for the induction as well as for the progression of ongoing aGVHD. This was tested by measuring preclinical efficacy of an anti-human OX40L monoclonal antibody (anti-hOX40L) in immunodeficient mice transplanted with human peripheral blood mononuclear cells (PBMCs). We also assessed the mechanisms by which anti-hOX40L suppresses aGVHD.

Materials and methods

Mice

Female NOG (NOD.Cg-Prkdc^{scid} Il2rg^{tm1Sug}/JicTac) mice (Taconic Biosciences) were housed in a specific pathogen-free environment at the animal facility. All experiments were performed under the protocol approved by the Mayo Clinic and Baylor Health Care System Institutional Animal Care and Use Committee. All mice received daily monitoring and care from the animal facility staff under the supervision of a veterinarian.

Xenogeneic aGVHD model and treatments

On day 0, female NOG mice (6-to-8 weeks old) received 1×10^7 freshly isolated human PBMCs via tail vein. PBMCs were isolated from buffy coats (Carter BloodCare) by density gradient centrifugation using Ficoll-Paque Plus (GE Healthcare). In a preventive mode, animals were given anti-hOX40L or IgG2b (10 μg per dose) intraperitoneally (i.p.) 3 times weekly from day 1 post-transplantation through week 3. In a therapeutic mode, animals were given anti-hOX40L or IgG2b (10 μg per dose) intraperitoneally 3 times weekly from day 21 post-transplantation through week 6. Clinical symptoms of aGVHD were graded according to published criteria (25). Peripheral blood was collected weekly after transplantation. aGVHD mice were euthanized in week 2 or week 4 post-transplantation. Liver, lung, spleen, skin, and gut tissues were collected for flow cytometry and histological analysis.

Anti-hOX40L generation and characterization

Mouse monoclonal antibody specific for human OX40L [19A3, IgG2b, GenBank accession number: MF589177 (www.ncbi.nlm.nih.gov/nuccore/MF589177.1) and MF589178 (www.ncbi.nlm.nih.gov/nuccore/MF589178.1) was generated in house as described previously (26). Recombinant fusion protein of hOX40L ectodomain and hIgG Fc (26) were expressed using the UCOE pCET-HS-puro vector system according to the manufacturer's protocol (Gibco), and purified by HiTrap protein A affinity chromatography (GE Healthcare). Anti-hOX40L (19A3, IgG2b) was purified by high-performance liquid chromatography using MabSelect SuRe HiTrap affinity column (GE Healthcare). The specificity of anti-hOX40L mAb was characterized by staining L cells transfected with hOX40L and by enzyme-linked immunosorbent assays (ELISAs) using plates coated with recombinant hOX40L ectodomain fused to hIgG Fc generated as previously described (26).

DC and T cell co-culture and cytokine assay

Blood myeloid DCs (mDCs) ($Lin^-HLA\text{-}DR^+CD11c^+CD123^-$) and allogeneic naïve $CD4^+$ T cells ($CD45RA^+CD45RO^-CCR7^+$) were sorted by FACSAria II (BD Biosciences). The purities of FACS-sortd cells were >99%. Total T cells, $CD4^+$, and $CD8^+$ T cells were isolated from PBMCs using enrichment kits (STEMCELL Technologies). Cells were cultured in a complete RPMI (cRPMI) 1640 medium containing 10% fetal calf serum (FCS, Gemini). cRPMI 1640 is composed of RPMI 1640 (Thermo Fisher Scientific) supplemented with 50 unit/mL penicillin, 50 μg/mL streptomycin, 2 mM L-glutamate, 1X non-essential amino acids, 1 mM sodium pyruvate (Sigma-Aldrich), and 25 mM HEPES (Thermo Fisher Scientific). mDCs were stimulated for 24h with 20 ng/mL thymic stromal lymphopoietin (TSLP) (27) and then washed. A total of 2×10^4/mL TSLP-mDCs were co-cultured for 7 days with 2×10^5/mL allogeneic T cells in the presence of anti-hOX40L or control antibody (5 μg/mL). T cells were then restimulated with Dynabeads human T-activator CD3/CD28 (Thermo Fisher Scientific) for 24h. T cell cytokine expression was assessed by intracellular cytokine staining as well as by multiplex bead-based assay (Millipore).

Tissue samples were homogenized and filtered through a 70 μm strainer. Human mononuclear cells (MNCs) were isolated by density-gradient centrifugation with Percoll (GE Healthcare). Cells were washed with cRPMI prior to analysis. Spleen cells were further treated with red blood cell (RBC) lysis buffer (Tonbo Biosciences). To assess intracellular

cytokine expression by T cells, cells were stimulated for 6h with phorbol 12-myristate 13-acetate (PMA, Sigma) at 25 μg/mL and ionomycin (Sigma) at 1 μg/mL in the presence of brefeldin A and monensin (BD Biosciences).

Antibodies, flow cytometry, and other reagents

Antibodies specific for CD3 (OKT3), CD8a (RPA-T8), CD123 (6H6), CD127 (A019D5), CD278 (ICOS, C398.4A), IL-21 (3A3-N2), TNF (MAb11), IL-4 (MP-425D2), IL-5 (JES1–39D10), IL-13 (JES10–5A2), HLA-DR (L243), CCR4 (L291H4), and linage cocktail were purchased from BioLegend. Antibodies specific for CD4 (RPA-T4), CD11c (B-ly6), CD19 (HIB19), CD25 (2A3), CD45 (HI30), CD56 (NCAM16.2), CD279 (PD-1, EH12.1), IL-17 (N49–653), and IFNγ (4S.B3) were from BD Biosciences. Antibodies specific for CD14 (61D3), IL-10 (JES3–9D7), CTLA-4 (14D3), and Foxp3 (PCH101) were from eBioscience. Anti-CXCR5 (51505) was from R&D Systems. Live/Dead Fixable dead cell stain kit and CellTrace CFSE Cell Proliferation kit were purchased from Invitrogen. Neutralizing anti-human IL-21 monoclonal antibody (anti-hIL-21) was generated as previously described (28). Etanercept was purchased from the pharmacy at Baylor University Medical Center. LSRFortessa (BD Biosciences) was used and flow cytometry data were analyzed with FlowJo v9 (FlowJo LLC).

U937-specific CTL generation and cytotoxicity assays

NOG mice with GVHD were i.p. injected with 1×10^7 γ-irradiated (30 Gy) U937 cells (ATCC) on days 0,7, and 14. GVHD mice were treated with anti-hOX40L or IgG2b at 10 μg per dose on days 1,3,5,8,10, and 12, and were euthanized on day 21. NOG mice with GVHD without i.p. injection of γ-irradiated U937 cells served as unimmunized control group. Human $CD8^+$ T cells were enriched from spleens using enrichment kits (STEMCELL Technologies). The purity of enriched $CD8^+$ T cells was >92%. $CD8^+$ T cells were cocultured with calcein AM-stained U937 cells at varying effector-to-target ratios for 4 h at 37°C. The fluorescence release into the supernatant by the lysed target cells was measured on a SpectraMax M2 (Molecular Devices). Percent lysis was calculated based on the background-subtracted test fluorescence relative to the maximum fluorescence without background. Background fluorescence was defined as spontaneous calcein AM release by the labeled U937 without any CTLs. Maximum fluorescence was defined as calcein AM release in the presence of 4% Triton-X 100 (Sigma) (29).

Statistics

Significance was determined in Prism 6.0h (GraphPad Software) using the analysis of variance (ANOVA) test for multiple comparison tests or Student's *t* test for two-group comparisons. Survival rates were analyzed by log-rank test using the Mantel-Cox method. *P* values < 0.05 were considered statistically significant.

Results

Anti-human OX40L monoclonal antibody

A mouse anti-hOX40L mAb (clone 19A3, IgG2b) was generated and its specificity was verified by staining hOX40L-expressing L cells (Fig. 1A) and ELISAs (Fig. 1B).

We next tested whether anti-hOX40L (19A3) is capable of modulating allogeneic $CD4^+$ T cell responses elicited with TSLP-treated mDCs. Fig. 1C shows that anti-hOX40L treatment resulted in decreased IL-5-, TNF-, IL-21-, and IFNg-producing $CD4^+$ T cell responses while it promotes IL-10-producing $CD4^+$ T cell responses. In support of the increase of IL-10-producing $CD4^+$ T cell responses, anti-hOX40L treatment increased the frequency of $CD25^+Foxp3^+CD127^{low}$ regulatory T cells (Tregs) (Fig. 1D).

Anti-hOX40L prevents the development of aGVHD with a gradual expansion of human leukocyte overtime

To test whether anti-hOX40L mAb could prevent the development of aGVHD, we employed a xenogeneic-aGVHD (x-aGVHD) model, where human T cells play a central role in the pathogenesis of aGVHD (30). GVHD development in this model is dependent upon human PBMC xeno-reactivity with mouse major histocompatibility (MHC) class I and class II (31–33). Following an i.v. injection of human PBMCs on day 0, animals received i.p. injections of either control IgG2b or anti-hOX40L mAb at indicated time points (Fig. 2A). The amount of antibody used in this study was pre-determined (Supplemental Fig. 1A). Anti-hOX40L treatment enhanced mouse survival at both 10 and 100 μg per dose. However, the frequency of human cells was significantly decreased at 100 μg per dose (Supplemental Fig. 1B). A dose of 10 μg was thus chosen for this study. Fig. 2A shows that mice treated with anti-hOX40L maintained and even gained body weight throughout the course of the experiment, while mice treated with IgG2b lost almost 20% of body weight by week 4. In addition, anti-hOX40L-treated mice exhibited a significantly increased overall survival rate (Fig. 2B). All mice treated with IgG2b developed aGVHD from week 2, but anti-hOX40L-treated mice were symptom free until week 8, 5 weeks after the last dose of anti-hOX40L (Fig. 2C).

Weekly analysis of circulating human leukocytes in the peripheral blood showed that human $CD45^+$ leukocytes were detected in all mice, and their frequency peaked in week 4 for IgG2b-treated mice and week 8 for anti-hOX40L-treated mice (Fig. 2D). Fig. 2E shows that the kinetics of the frequency of $CD3^+$ cells closely resembled that of $CD45^+$ cells. Accordingly, the majority (>70%) of the human $CD45^+$ cells in the blood of aGVHD mice were $CD3^+$ (Fig. 2F), as previously reported (34, 35). Whereas the frequency of circulating human $CD4^+$ T cells remained comparable in the two groups for the first 2 weeks post-transplantation, anti-hOX40L-treated mice displayed a sustained blood $CD4^+$ T cells week 3 (Supplemental Fig. 2A). The frequency of $CD8^+$ T cells from anti-hOX40L-treated mice was lower than that of their IgG2b-treated mice in week 3 (Supplemental Fig. 2B). The percentages of human $CD19^+$ B cells, $CD14^+$ monocytes, and $CD3^-CD56^+$ NK cells all decreased over time in the two groups (Supplemental Fig. 2C–E). Taken together, these results show that anti-hOX40L treatment can effectively prevent the development of aGVHD in the x-aGVHD model. Mice treated with anti-hOX40L had decreased engraftment of human T cells at an early time point, but it expanded over time without showing aGVHD symptoms.

OX40L blockade reduces human leukocyte infiltration into target tissues

Tissue damage in target organs caused by human lymphocytes in aGVHD models is mainly due to an infiltration of human lymphocytes and cytokine storm (36, 37). We therefore

analyzed human leukocyte infiltration in the liver, lung, and spleen of recipient mice on week 4 before control mice died. As shown in Fig. 3A, the absolute numbers of MNCs isolated from the livers of anti-hOX40L-treated mice were significantly lower than those from the IgG2b-treated mice. However, this was not the case in the lungs or spleens. Further analysis of single-cell suspensions of the target tissues shows that anti-hOX40L-treated mice had a significantly lower infiltration rate of human $CD45^+$ cells in the livers, lungs, and spleens than IgG2b-treated mice (Fig. 3B). Anti-hOX40L treatment did not significantly alter human $CD4^+$ T cell infiltration in the livers, but it decreased $CD8^+$ T cell infiltration (Fig. 3C). Immunohistochemistry data (Fig. 3D) further demonstrated that anti-hOX40L treatment could decrease $CD8^+$ T cell infiltration in the livers. Livers of the IgG2b-treated animals were heavily infiltrated by human $CD45^+$ cells, including $CD3^+$ T cells, whereas anti-hOX40L treatment decreased the infiltration of these cells. Anti-hOX40L treatment also resulted in decreased infiltration of $CD45^+$, $CD3^+$, $CD4^+$, $CD8^+$ cells in both guts and skin (Supplemental Fig. 3). Taken together, these data (Fig. 3 and Supplemental Fig. 3) suggest that anti-hOX40L treatment reduces human T cell infiltration in the aGVHD target organs.

Anti-hOX40L treatment reduces inflammatory T cell responses while promoting Treg responses in aGVHD mice

To further understand the mechanisms whereby anti-hOX40L treatment ameliorates x-aGVHD, we first investigated OX40L expression by DCs and T cells. As shown in Fig. 4A, during x-aGVHD, OX40L-expressing $CD1c^+$ cells closely interacted with T cells in the spleens. Interestingly, the majority of T cells in the spleens also expressed OX40L as well, as previously described (38).

We next investigated the cytokine expression profiles of splenic T cells from the two groups of mice on week 4. As shown in Fig. 4B, anti-hOX40L treatment resulted in the enhancement of IL-10-producing $CD4^+$ T cell responses, whereas it decreased IL-21-, TNF-, and IFNg-producing $CD4^+$ T cell responses. Such decreases were similarly observed in $CD8^+$ T cell responses (Fig. 4C). In line with the increase of IL-10^+ $CD4^+$ T cell responses (Fig. 4B), anti-hOX40L treatment also increased the frequency of $CD25^+Foxp3^+CD127^{lo}$CTLA-4^+CCR4^+ Tregs (Fig. 4D) (39). Anti-hOX40L treatment also resulted in decreased expression of PD-1 on the surface of $CXCR5^+ICOS^+CD4^+$ follicular helper T (Tfh) cells (Fig. 4E).

We also investigated the cytokine expression profiles of T cells from both livers and lungs from the two groups of animals (Supplemental Fig. 4). Anti-hOX40L-treated mice had less abundant IL-21^+ and IFNγ^+CD4^+ T cells (Supplemental Fig. 4A) in the livers as well as in the lungs (Supplemental Fig. 4B). Anti-hOX40L treatment also resulted in decreased frequency of IL-21^+, TNF^+, and IFNγ^+ $CD8^+$ T cells in the livers (Supplemental Fig. 4C) and lungs (Supplemental Fig. 4D). Although the differences were not statistically significant, there was a tendency toward increased IL-10^+CD4^+ T cells in both livers and lungs (Supplemental Fig. 4A–B) from anti-hOX40L-treated mice, when compared with control mice. Similar to the splenic Tfh cells (Fig. 4E), $CXCR5^+ICOS^+CD4^+$ T cells from both livers (Supplemental Fig. 4E) and lungs (Supplemental Fig. 4F) of animals treated with anti-hOX40L-treated mice showed decreased surface PD-1 expression, which is consistent

with the decrease in IL-21$^+$CD4$^+$ T cells (Supplemental Fig. 4A–B). Taken together, our data (Fig. 4 and Supplemental Fig. 4) demonstrate that anti-hOX40L treatment promotes Treg responses while decreasing inflammatory T cell responses, which can suppress the development of x-aGVHD. The frequency of Th2 and Th17 cells were too low to determine the effects of anti-hOX40L treatment.

Anti-hOX40L is more effective than the combination of etanercept and anti-hIL-21 in preventing aGVHD

Both TNF and IL-21 contribute to the pathogenesis of aGVHD (1, 40, 41). Our data show that anti-hOX40L treatment decreases both TNF- and IL-21-producing T cell responses. We thus compared anti-hOX40L with combination of etanercept and anti-hIL-21 for their ability to suppress aGVHD manifestations. Fig. 5A shows that anti-hOX40L-treated mice did not show a significant weight loss overtime, while IgG2b-treated mice started losing body weight after week 3. Significant body weight loss and progressive disease severity were also observed after week 4, a week after the final treatment, for the mice that received the combination of etanercept and anti-hIL-21 (Fig. 5B), with only half of the mice alive by the end of week 6 (Fig. 5C). In contrast, anti-hOX40L-treated mice had a survival rate of 100% up to week 6 and remained free of aGVHD symptoms (Fig. 5B–C). Taken together, these data indicate that IL-21 and TNF contribute to aGVHD, as previously reported (1, 42–44). Nonetheless, anti-hOX40L is more efficient than the combination of etanercept and anti-hIL-21 in ameliorating aGVHD symptoms, which could be supported with the enhanced Treg responses by anti-hOX40L treatment. These data also demonstrate that immune modulation with anti-hOX40L results in better and more sustained outcomes than blocking such soluble cytokines.

Anti-hOX40L treatment does not impair cytolytic activity of CD8$^+$ T cell

We next tested whether anti-hOX40L treatment could interfere with cytolytic activity of CD8$^+$ T cells. As presented in Fig. 6A, aGVHD mice were immunized with γ-irradiated U937 cells, a human histolytic lymphoma cell line, on day 0, and boosted on days 7 and 14 (29), while they were treated with anti-hOX40L three times a week for 2 weeks. On day 21, splenic CD8$^+$ T cells were tested for their cytolytic activities using calcein-acetoxymethyl (calcein AM)-stained U937 cells. As shown in Fig. 6B, CD8$^+$ T cells from anti-hOX40L-treated mice displayed no compromises in their killing capacity against U937 target cells when compared with mice treated with IgG2b. CD8$^+$ T cells from unimmunized animals did not lyse U937 cells. These data suggest that anti-hOX40L treatment efficiently suppresses x-aGVHD, while it does not interfere with cytolytic activity of CD8$^+$ T cells.

Anti-hOX40L treatment can suppress an established aGVHD

We next assessed therapeutic efficacy of anti-hOX40L in mice with mild to severe aGVHD. aGVHD mice were injected i.p. with either anti-hOX40L or IgG2b starting from day 21 when mice already exhibited mild-to-severe aGVHD symptoms. Administration of anti-hOX40L stabilized the average body weight and significantly reduced aGVHD-related lethality compared with the IgG2b-treated group during the course of the study (Fig. 7A–B). Anti-hOX40L treatment kept the clinical manifestations of aGVHD in check and even

alleviated the symptoms shortly after the treatment started in week 3 (Fig. 7C). These data suggest that anti-hOX40L treatment is able to manage ongoing aGVHD.

Discussion

This study demonstrates that the interaction between OX40L and OX40 is a critical component not only for the induction of aGVHD, but also for the progression of aGVHD. Accordingly, blocking the interaction between OX40L and OX40 with anti-hOX40L antibody can effectively prevent and treat x-aGVHD that is caused mainly by human T cells. In addition, this study also extends previous works performed in animals (16, 17) by providing mechanisms whereby hOX40L blockade ameliorate aGVHD manifestations without compromising cytolytic activity of $CD8^+$ T cells.

Our results highlight the significant effects of OX40L blockade on preventing aGVHD associated organ damage and lethality. Treatment with anti-hOX40L markedly reduced human $CD45^+$ cell infiltration in aGVHD target tissues such as skin, liver, lung, and intestine. Interestingly, anti-hOX40L treatment did not significantly alter the frequency of $CD4^+$ T cells infiltration in the target organs tested. However, anti-hOX40L treatment resulted in significant decreases of $CD8^+$ T cell infiltration in the target organs especially livers and lungs. These data may indicate the roles of $CD8^+$ T cells in the pathogenesis of aGVHD (30, 40, 45, 46).

In addition to the reduced infiltration of T cells in target organs, anti-hOX40L treatment resulted in decreases of IL-21-, TNF-, and IFNg-producing $CD4^+$ and $CD8^+$ T cell responses overall, although the levels of significance are variable in different tissues. The decrease of Tfh responses by anti-hOX40L treatment was also supported by the finding that PD-1 expression levels (47–50) on Tfh cells ($CD4^+CXCR5^+ICOS^+$) in target organs and spleen are significantly decreased by anti-hOX40L treatment.

More importantly, anti-hOX40L treatment resulted in increases of IL-10-producing $CD4^+$ T cell responses, which is in line with the increased frequency of Tregs ($CD4^+CD25^+FoxP3^+CD127^{low}CTLA\text{-}4^+CCR4^+$) in spleen and other tissues. In addition to the decreased proinflammatory T cell responses, such increases of Tregs expressing IL-10 in the target organs might also play critical roles in the preclinical outcomes of anti-hOX40L treatments (22, 24, 51–53). Sustained role of Tregs in the suppression of aGVHD can be further supported by the fact that animals received anti-hOX40L treatment for 3 weeks did not develop aGVHD until the end of experiment (week 8). Although the duration of treatment was specifically designed becuase human APCs were detectable up to 3 weeks post-transplantation and waned overtime, in order to gain a long-term tolerance, prolonged treatment with anti-hOX40L may take into account in clinical practice in bone marrow transplantation due to immune reconstitution.

In one of our ongoing study, we have further found that anti-hOX40L treatment can indeed promote allo-antigen-specific Treg responses *in vitro* (data not shown). Importantly, the increased frequency of functional Tregs in mice treated with anti-hOX40L did not interfere

with cytolytic activity of $CD8^+$ T cells, suggesting that GVL and antigen-specific memory $CD8^+$ T cell responses are still achievable.

Another notable finding of our studies was that blocking OX40L increases $CCR4^+$ expression on $CD4^+$ Tregs, indicating the migration capacity of Tregs to nonlymphoid tissues such as skin and lung (51). Interestingly, it has been reported that the pre-transplantation use of mogamulizumab, an anti-CCR4 monoclonal antibody that was recently approved in Japan as a treatment for aggressive adult T cell leukemia/lymphoma, significantly increases the risks of severe and corticosteroid-refractory aGVHD (53). These results may support the importance of CCR4-expressing Tregs in controlling aGVHD.

Activated T cells can also express OX40L (54, 55). We also found that OX40L expression by $CD3^+$ T cells was readily detectable in x-aGVHD mice. Therefore, we cannot rule out the effect of anti-hOX40L treatments on the potential roles of $OX40L^+$ T cells in the pathogenesis of aGVHD. Although no differences were observed between T cells from $OX40L^{-/-}$ and wild-type mice in a primary MLR *in vitro* or *in vivo* (17), a human *in vitro* study suggested that anti-hOX40L reduces the proliferation of donor $CD4^+$ T cells stimulated by purified $OX40L^{-/-}$ mature DCs (54). In this study, we noticed that high doses of anti-OX40L treatment resulted in enhanced animal survivals, but this is probably due to the decrease of human cell infiltration. We thus performed experiments with 10 μg per dose which provided a minimal impact on the frequency of circulating human $CD45^+$ cells in the blood, while retaining maximal protection from aGVHD-induced lethality. Even with this low amount of anti-hOX40L antibody (10 ug per dose), when compared to anti-IL-21 (100 ug per dose) and etanercept (200 ug per dose), we still can not rule out an antibody dependent cell-mediated cytotoxicity. However, this question may need to be properly addressed when anti-hOX40L antibody is humanized for clinical usages.

In conclusion, this study demonstrates that the interaction between OX40L-OX40 is critical importance for both the induction and progression of aGVHD caused by human T cells. Data from this study further demonstrate that blocking OX40L-OX40 interaction promotes Treg responses followed by an amelioration of aGVHD manifestation without interfering with $CD8^+$ T cell functions. This study also strongly supports clinical development of anti-hOX40L as a novel therapy for aGVHD, especially for patients with residual and relapsing hematological malignancies after allogeneic HSCT.

Supplementary Material

Refer to Web version on PubMed Central for supplementary material.

Acknowledgments

We thank the Flow Cytometry Core Laboratory, Sample Procurement Core Laboratory, and Bioscience Center at Baylor Scott & White Research Institute for assisting with work performed in this study.

This work was supported by Mayo Clinic (H.J. and S.O.), Baylor Sammons Cancer Center Grant (H.J.), and NIH 1 R01 AI 105066 (S.O.).

Abbreviations used in this article:

aGVHD	acute graft-versus-host disease
anti-hIL-21	Anti-human IL-21 monoclonal antibody
anti-hOX40L	anti-human OX40L monoclonal antibody
mDC	myeloid dendritic cells
MNCs	mononuclear cells
NOG	NOD.Cg-Prkdc^{scid} Il2rg^{tm1Sug}/JicTac
Tfh	T follicular helper
Treg	Regulatory T cell
X-aGVHD	Xenegeneic acute graft-versus-host disease

References

1. Bucher C, Koch L, Vogtenhuber C, Goren E, Munger M, Panoskaltsis-Mortari A, Sivakumar P, and Blazar BR. 2009 IL-21 blockade reduces graft-versus-host disease mortality by supporting inducible T regulatory cell generation. Blood 114: 5375–5384. [PubMed: 19843883]
2. Storb R, Antin JH, and Cutler C. 2010 Should methotrexate plus calcineurin inhibitors be considered standard of care for prophylaxis of acute graft-versus-host disease? Biol Blood Marrow Transplant 16: S18–27. [PubMed: 19857584]
3. Ruutu T, van Biezen A, Hertenstein B, Henseler A, Garderet L, Passweg J, Mohty M, Sureda A, Niederwieser D, Gratwohl A, and de Witte T. 2012 Prophylaxis and treatment of GVHD after allogeneic haematopoietic SCT: a survey of centre strategies by the European Group for Blood and Marrow Transplantation. Bone Marrow Transplant 47: 1459–1464. [PubMed: 22410750]
4. Chao NJ, Schmidt GM, Niland JC, Amylon MD, Dagis AC, Long GD, Nademanee AP, Negrin RS, O'Donnell MR, Parker PM, and et al. 1993 Cyclosporine, methotrexate, and prednisone compared with cyclosporine and prednisone for prophylaxis of acute graft-versus-host disease. The New England journal of medicine 329: 1225–1230. [PubMed: 8413388]
5. Marcen R 2009 Immunosuppressive drugs in kidney transplantation: impact on patient survival, and incidence of cardiovascular disease, malignancy and infection. Drugs 69: 2227–2243. [PubMed: 19852526]
6. Deeg HJ 2007 How I treat refractory acute GVHD. Blood 109: 4119–4126. [PubMed: 17234737]
7. Ahmadi SM, Holzl MA, Mayer E, Wekerle T, and Heitger A. 2014 CTLA4-Ig preserves thymus-derived T regulatory cells. Transplantation 98: 1158–1164. [PubMed: 25269023]
8. Seldon TA, Pryor R, Palkova A, Jones ML, Verma ND, Findova M, Braet K, Sheng Y, Fan Y, Zhou EY, Marks JD, Munro T, Mahler SM, Barnard RT, Fromm PD, Silveira PA, Elgundi Z, Ju X, Clark GJ, Bradstock KF, Munster DJ, and Hart DN. 2016 Immunosuppressive human anti-CD83 monoclonal antibody depletion of activated dendritic cells in transplantation. Leukemia 30: 692–700. [PubMed: 26286117]
9. Sondergaard H, Kvist PH, and Haase C. 2013 Human T cells depend on functional calcineurin, tumour necrosis factor-alpha and CD80/CD86 for expansion and activation in mice. Clin Exp Immunol 172: 300–310. [PubMed: 23574326]
10. Collin MP, Munster D, Clark G, Wang X-N, Dickinson AM, and Hart DN. 2005 In Vitro Depletion of Tissue-Derived Dendritic Cells by CMRF-44 Antibody and Alemtuzumab: Implications for the Control of Graft-Versus-Host Disease. Transplantation 79: 722–725. [PubMed: 15785380]

11. Burrows KE, Dumont C, Thompson CL, Catley MC, Dixon KL, and Marshall D. 2015 OX40 blockade inhibits house dust mite driven allergic lung inflammation in mice and in vitro allergic responses in humans. Eur J Immunol 45: 1116–1128. [PubMed: 25545270]
12. Elhai M, Avouac J, Hoffmann-Vold AM, Ruzehaji N, Amiar O, Ruiz B, Brahiti H, Ponsoye M, Frechet M, Burgevin A, Pezet S, Sadoine J, Guilbert T, Nicco C, Akiba H, Heissmeyer V, Subramaniam A, Resnick R, Molberg O, Kahan A, Chiocchia G, and Allanore Y. 2016 OX40L blockade protects against inflammation-driven fibrosis. Proc Natl Acad Sci U S A 113: E3901–3910. [PubMed: 27298374]
13. Gwyer Findlay E, Danks L, Madden J, Cavanagh MM, McNamee K, McCann F, Snelgrove RJ, Shaw S, Feldmann M, Taylor PC, Horwood NJ, and Hussell T. 2014 OX40L blockade is therapeutic in arthritis, despite promoting osteoclastogenesis. Proc Natl Acad Sci U S A 111: 2289–2294. [PubMed: 24469824]
14. Ndhlovu LC, Ishii N, Murata K, Sato T, and Sugamura K. 2001 Critical Involvement of OX40 Ligand Signals in the T Cell Priming Events During Experimental Autoimmune Encephalomyelitis. The Journal of Immunology 167: 2991–2999. [PubMed: 11509650]
15. Nohara C, Akiba H, Nakajima A, Inoue A, Koh CS, Ohshima H, Yagita H, Mizuno Y, and Okumura K. 2001 Amelioration of Experimental Autoimmune Encephalomyelitis with Anti-OX40 Ligand Monoclonal Antibody: A Critical Role for OX40 Ligand in Migration, But Not Development, of Pathogenic T Cells. The Journal of Immunology 166: 2108–2115. [PubMed: 11160262]
16. Tsukada N, Akiba H, Kobata T, Aizawa Y, Yagita H, and Okumura K. 2000 Blockade of CD134 (OX40)-CD134L interaction ameliorates lethal acute graft-versus-host disease in a murine model of allogeneic bone marrow transplantation. Blood 95: 2434–2439. [PubMed: 10733518]
17. Blazar BR, Sharpe AH, Chen AI, Panoskaltsis-Mortari A, Lees C, Akiba H, Yagita H, Killeen N, and Taylor PA. 2003 Ligation of OX40 (CD134) regulates graft-versus-host disease (GVHD) and graft rejection in allogeneic bone marrow transplant recipients. Blood 101: 3741–3748. [PubMed: 12521997]
18. Tkachev V, Furlan SN, Watkins B, Hunt DJ, Zheng HB, Panoskaltsis-Mortari A, Betz K, Brown M, Schell JB, Zeleski K, Yu A, Kirby I, Cooley S, Miller JS, Blazar BR, Casson D, Bland-Ward P, and Kean LS. 2017 Combined OX40L and mTOR blockade controls effector T cell activation while preserving Treg reconstitution after transplant. Science translational medicine 9.
19. Huang Y, Feng S, Tang R, Du B, Xu K, and Pan X. 2010 Efficacy of pretreatment of allografts with methoxypolyethylene glycol-succinimidyl-propionic acid ester in combination with an anti-OX40L monoclonal antibody in relieving graft-versus-host disease in mice. International journal of hematology 92: 609–616. [PubMed: 20953915]
20. Ito T, Wang YH, Duramad O, Hanabuchi S, Perng OA, Gilliet M, Qin FX, and Liu YJ. 2006 OX40 ligand shuts down IL-10-producing regulatory T cells. Proc Natl Acad Sci U S A 103: 13138–13143. [PubMed: 16924108]
21. Pedroza-Gonzalez A, Xu K, Wu TC, Aspord C, Tindle S, Marches F, Gallegos M, Burton EC, Savino D, Hori T, Tanaka Y, Zurawski S, Zurawski G, Bover L, Liu YJ, Banchereau J, and Palucka AK. 2011 Thymic stromal lymphopoietin fosters human breast tumor growth by promoting type 2 inflammation. J Exp Med 208: 479–490. [PubMed: 21339324]
22. Ito T, Wang YH, Duramad O, Hori T, Delespesse GJ, Watanabe N, Qin FX, Yao Z, Cao W, and Liu YJ. 2005 TSLP-activated dendritic cells induce an inflammatory T helper type 2 cell response through OX40 ligand. J Exp Med 202: 1213–1223. [PubMed: 16275760]
23. Joo H, Upchurch K, Zhang W, Ni L, Li D, Xue Y, Li XH, Hori T, Zurawski S, Liu YJ, Zurawski G, and Oh S. 2015 Opposing Roles of Dectin-1 Expressed on Human Plasmacytoid Dendritic Cells and Myeloid Dendritic Cells in Th2 Polarization. J Immunol 195: 1723–1731. [PubMed: 26123355]
24. Morita R, Schmitt N, Bentebibel SE, Ranganathan R, Bourdery L, Zurawski G, Foucat E, Dullaers M, Oh S, Sabzghabaei N, Lavecchio EM, Punaro M, Pascual V, Banchereau J, and Ueno H. 2011 Human blood CXCR5(+)CD4(+) T cells are counterparts of T follicular cells and contain specific subsets that differentially support antibody secretion. Immunity 34: 108–121. [PubMed: 21215658]

25. Cooke KR, Kobzik L, Martin TR, Brewer J, Delmonte J Jr., Crawford JM, and Ferrara JL. 1996 An experimental model of idiopathic pneumonia syndrome after bone marrow transplantation: I. The roles of minor H antigens and endotoxin. Blood 88: 3230–3239. [PubMed: 8963063]

26. Ni L, Gayet I, Zurawski S, Duluc D, Flamar AL, Li XH, O'Bar A, Clayton S, Palucka AK, Zurawski G, Banchereau J, and Oh S. 2010 Concomitant activation and antigen uptake via human dectin-1 results in potent antigen-specific CD8+ T cell responses. J Immunol 185: 3504–3513. [PubMed: 20729328]

27. Soumelis V, Reche PA, Kanzler H, Yuan W, Edward G, Homey B, Gilliet M, Ho S, Antonenko S, Lauerma A, Smith K, Gorman D, Zurawski S, Abrams J, Menon S, McClanahan T, de Waal-Malefyt Rd R, Bazan F, Kastelein RA, and Liu YJ. 2002 Human epithelial cells trigger dendritic cell mediated allergic inflammation by producing TSLP. Nat Immunol 3: 673–680. [PubMed: 12055625]

28. Schmitt N, Morita R, Bourdery L, Bentebibel SE, Zurawski SM, Banchereau J, and Ueno H. 2009 Human dendritic cells induce the differentiation of interleukin-21-producing T follicular helper-like cells through interleukin-12. Immunity 31: 158–169. [PubMed: 19592276]

29. Betts BC, Veerapathran A, Pidala J, Yang H, Horna P, Walton K, Cubitt CL, Gunawan S, Lawrence HR, Lawrence NJ, Sebti SM, and Anasetti C. 2017 Targeting Aurora kinase A and JAK2 prevents GVHD while maintaining Treg and antitumor CTL function. Science translational medicine 9.

30. van Rijn RS, Simonetti ER, Hagenbeek A, Hogenes MC, de Weger RA, Canninga-van Dijk MR, Weijer K, Spits H, Storm G, van Bloois L, Rijkers G, Martens AC, and Ebeling SB. 2003 A new xenograft model for graft-versus-host disease by intravenous transfer of human peripheral blood mononuclear cells in RAG2−/− gammac−/− double-mutant mice. Blood 102: 2522–2531. [PubMed: 12791667]

31. Tary-Lehmann M, Lehmann PV, Schols D, Roncarolo MG, and Saxon A. 1994 Anti-SCID mouse reactivity shapes the human CD4+ T cell repertoire in hu-PBL-SCID chimeras. J Exp Med 180: 1817–1827. [PubMed: 7964463]

32. King MA, Covassin L, Brehm MA, Racki W, Pearson T, Leif J, Laning J, Fodor W, Foreman O, Burzenski L, Chase TH, Gott B, Rossini AA, Bortell R, Shultz LD, and Greiner DL. 2009 Human peripheral blood leucocyte non-obese diabetic-severe combined immunodeficiency interleukin-2 receptor gamma chain gene mouse model of xenogeneic graft-versus-host-like disease and the role of host major histocompatibility complex. Clin Exp Immunol 157: 104–118. [PubMed: 19659776]

33. Ito R, Katano I, Kawai K, Yagoto M, Takahashi T, Ka Y, Ogura T, Takahashi R, and Ito M. 2017 A Novel Xenogeneic Graft-Versus-Host Disease Model for Investigating the Pathological Role of Human CD4(+) or CD8(+) T Cells Using Immunodeficient NOG Mice. Am J Transplant 17: 1216–1228. [PubMed: 27862942]

34. Ali N, Flutter B, Sanchez Rodriguez R, Sharif-Paghaleh E, Barber LD, Lombardi G, and Nestle FO. 2012 Xenogeneic graft-versus-host-disease in NOD-scid IL-2Rgammanull mice display a T-effector memory phenotype. PLoS One 7: e44219. [PubMed: 22937164]

35. King M, Pearson T, Shultz LD, Leif J, Bottino R, Trucco M, Atkinson MA, Wasserfall C, Herold KC, Woodland RT, Schmidt MR, Woda BA, Thompson MJ, Rossini AA, and Greiner DL. 2008 A new Hu-PBL model for the study of human islet alloreactivity based on NOD-scid mice bearing a targeted mutation in the IL-2 receptor gamma chain gene. Clin Immunol 126: 303–314. [PubMed: 18096436]

36. Ferrara JL, Levine JE, Reddy P, and Holler E. 2009 Graft-versus-host disease. Lancet (London, England) 373: 1550–1561.

37. Blazar BR, Murphy WJ, and Abedi M. 2012 Advances in graft-versus-host disease biology and therapy. Nat Rev Immunol 12: 443–458. [PubMed: 22576252]

38. Mendel I, and Shevach EM. 2006 Activated T cells express the OX40 ligand: requirements for induction and costimulatory function. Immunology 117: 196–204. [PubMed: 16423055]

39. Sugiyama D, Nishikawa H, Maeda Y, Nishioka M, Tanemura A, Katayama I, Ezoe S, Kanakura Y, Sato E, Fukumori Y, Karbach J, Jager E, and Sakaguchi S. 2013 Anti-CCR4 mAb selectively depletes effector-type FoxP3+CD4+ regulatory T cells, evoking antitumor immune responses in humans. Proc Natl Acad Sci U S A 110: 17945–17950. [PubMed: 24127572]

40. Hippen KL, Bucher C, Schirm DK, Bearl AM, Brender T, Mink KA, Waggie KS, Peffault de Latour R, Janin A, Curtsinger JM, Dillon SR, Miller JS, Socie G, and Blazar BR. 2012 Blocking

IL-21 signaling ameliorates xenogeneic GVHD induced by human lymphocytes. Blood 119: 619–628. [PubMed: 22077059]

41. Levine JE, Paczesny S, Mineishi S, Braun T, Choi SW, Hutchinson RJ, Jones D, Khaled Y, Kitko CL, Bickley D, Krijanovski O, Reddy P, Yanik G, and Ferrara JL. 2008 Etanercept plus methylprednisolone as initial therapy for acute graft-versus-host disease. Blood 111:2470–2475. [PubMed: 18042798]
42. Meguro A, Ozaki K, Oh I, Hatanaka K, Matsu H, Tatara R, Sato K, Leonard WJ, and Ozawa K. 2010 IL-21 is critical for GVHD in a mouse model. Bone Marrow Transplant 45: 723–729. [PubMed: 19718060]
43. Brown GR, Lindberg G, Meddings J, Silva M, Beutler B, and Thiele D. 1999 Tumor necrosis factor inhibitor ameliorates murine intestinal graft-versus-host disease. Gastroenterology 116: 593–601. [PubMed: 10029618]
44. Hill GR, and Ferrara JL. 2000 The primacy of the gastrointestinal tract as a target organ of acute graft-versus-host disease: rationale for the use of cytokine shields in allogeneic bone marrow transplantation. Blood 95: 2754–2759. [PubMed: 10779417]
45. Hanash AM, Kappel LW, Yim NL, Nejat RA, Goldberg GL, Smith OM, Rao UK, Dykstra L, Na IK, Holland AM, Dudakov JA, Liu C, Murphy GF, Leonard WJ, Heller G, and van den Brink MR. 2011 Abrogation of donor T-cell IL-21 signaling leads to tissue-specific modulation of immunity and separation of GVHD from GVL. Blood 118: 446–455. [PubMed: 21596854]
46. Hatano R, Ohnuma K, Yamamoto J, Dang NH, Yamada T, and Morimoto C. 2013 Prevention of acute graft-versus-host disease by humanized anti-CD26 monoclonal antibody. Br J Haematol 162: 263–277. [PubMed: 23692598]
47. He J, Tsai LM, Leong YA, Hu X, Ma CS, Chevalier N, Sun X, Vandenberg K, Rockman S, Ding Y, Zhu L, Wei W, Wang C, Karnowski A, Belz GT, Ghali JR, Cook MC, Riminton DS, Veillette A, Schwartzberg PL, Mackay F, Brink R, Tangye SG, Vinuesa CG, Mackay CR, Li Z, and Yu D. 2013 Circulating precursor CCR7(lo)PD-1(hi) CXCR5(+) CD4(+) T cells indicate Tfh cell activity and promote antibody responses upon antigen reexposure. Immunity 39: 770–781. [PubMed: 24138884]
48. Shi J, Hou S, Fang Q, Liu X, Liu X, and Qi H. 2018 PD-1 Controls Follicular T Helper Cell Positioning and Function. Immunity 49: 264–274.e264. [PubMed: 30076099]
49. Havenith SH, Remmerswaal EB, Idu MM, van KA Donselaar-van der Pant N van der Bom FJ Bemelman EM van Leeuwen IJ ten Berge, and van Lier RA. 2014 CXCR5+CD4+ follicular helper T cells accumulate in resting human lymph nodes and have superior B cell helper activity. Int Immunol 26: 183–192. [PubMed: 24291746]
50. Liu D, Liu J, Wang J, Liu C, Yang S, and Jiang Y. 2016 Distinct phenotypic subpopulations of circulating CD4(+)CXCR5(+) follicular helper T cells in children with active IgA vasculitis. BMC Immunol 17: 40. [PubMed: 27769184]
51. Sather BD, Treuting P, Perdue N, Miazgowicz M, Fontenot JD, Rudensky AY, and Campbell DJ. 2007 Altering the distribution of Foxp3(+) regulatory T cells results in tissue-specific inflammatory disease. J Exp Med 204: 1335–1347. [PubMed: 17548521]
52. Feng G, Nadig SN, Backdahl L, Beck S, Francis RS, Schiopu A, Whatcott A, Wood KJ, and Bushell A. 2011 Functional regulatory T cells produced by inhibiting cyclic nucleotide phosphodiesterase type 3 prevent allograft rejection. Science translational medicine 3: 83ra40.
53. Fuji S, Inoue Y, Utsunomiya A, Moriuchi Y, Uchimaru K, Choi I, Otsuka E, Henzan H, Kato K, Tomoyose T, Yamamoto H, Kurosawa S, Matsuoka K, Yamaguchi T, and Fukuda T. 2016 Pretransplantation Anti-CCR4 Antibody Mogamulizumab Against Adult T-Cell Leukemia/Lymphoma Is Associated With Significantly Increased Risks of Severe and Corticosteroid-Refractory Graft-Versus-Host Disease, Nonrelapse Mortality, and Overall Mortality. J Clin Oncol 34: 3426–3433. [PubMed: 27507878]
54. Ukyo N, Hori T, Yanagita S, Ishikawa T, and Uchiyama T. 2003 Costimulation through OX40 is crucial for induction of an alloreactive human T-cell response. Immunology 109: 226–231. [PubMed: 12757617]
55. Kobbe G, Schneider P, Rohr U, Fenk R, Neumann F, Aivado M, Dietze L, Kronenwett R, Hunerliturkoglu A, and Haas R. 2001 Treatment of severe steroid refractory acute graft-versus-

host disease with infliximab, a chimeric human/mouse antiTNFalpha antibody. Bone Marrow Transplant 28: 47–49. [PubMed: 11498743]

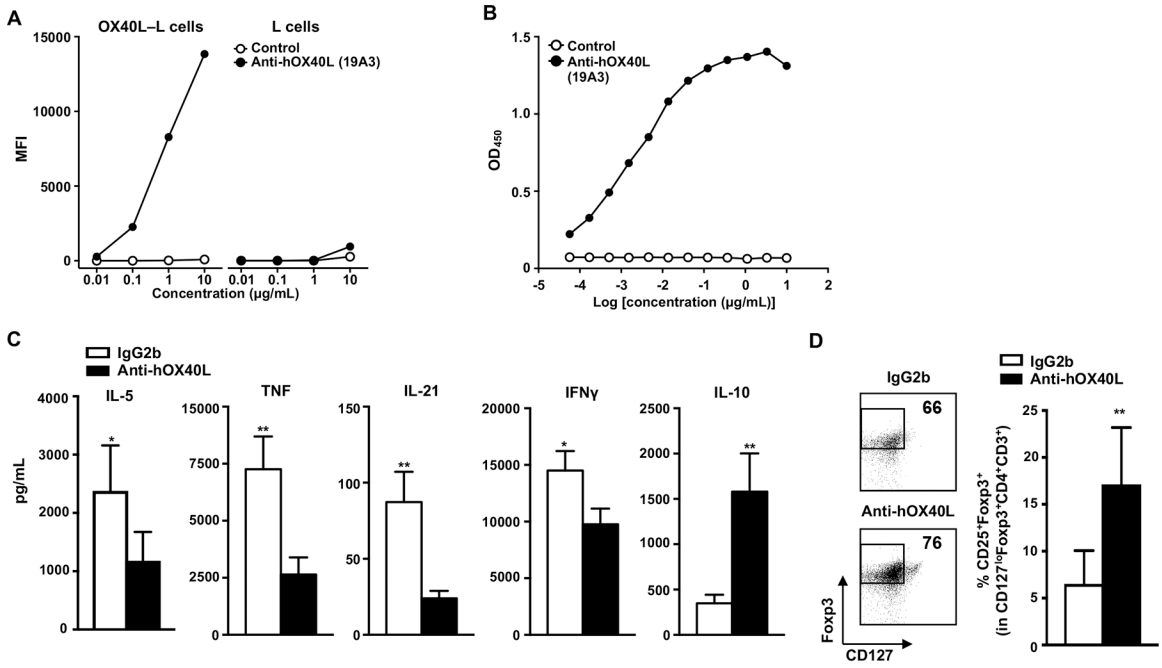

Figure 1. Anti-hOX40L decreases IL-5-, TNF-, IL-21, and IFNg-producing CD4$^+$ T cell responses, but increases IL-10-producing regulatory CD4$^+$ T cell responses.

(A) Assessment of anti-hOX40L antibody binding to hOX40L-expressing L cells (left) or L cells (right) by flow cytometry. **(B)** Assessment of anti-hOX40L antibody specificity by ELISA using plates coated with hOX40L protein. Data are representative from three independent experiments. **(C)** Allogeneic naïve CD4$^+$ T cells were co-cultured with TSLP-treated mDCs for 7 days in the presence of anti-hOX40L or control antibody. T cells were restimulated overnight with anti-human CD3/28 beads. The amount of cytokines secreted from T cells were measured by a bead-based multiplex assay, **(D)** Analysis of the frequency of CD4$^+$ Tregs by flow cytometry. All data are representative of at least three independent experiments. Error bars represent mean ± SD of quadruplicate assays. *P* values were determined with unpaired Student's *t* test. **P* < 0.05, ***P* < 0.01.

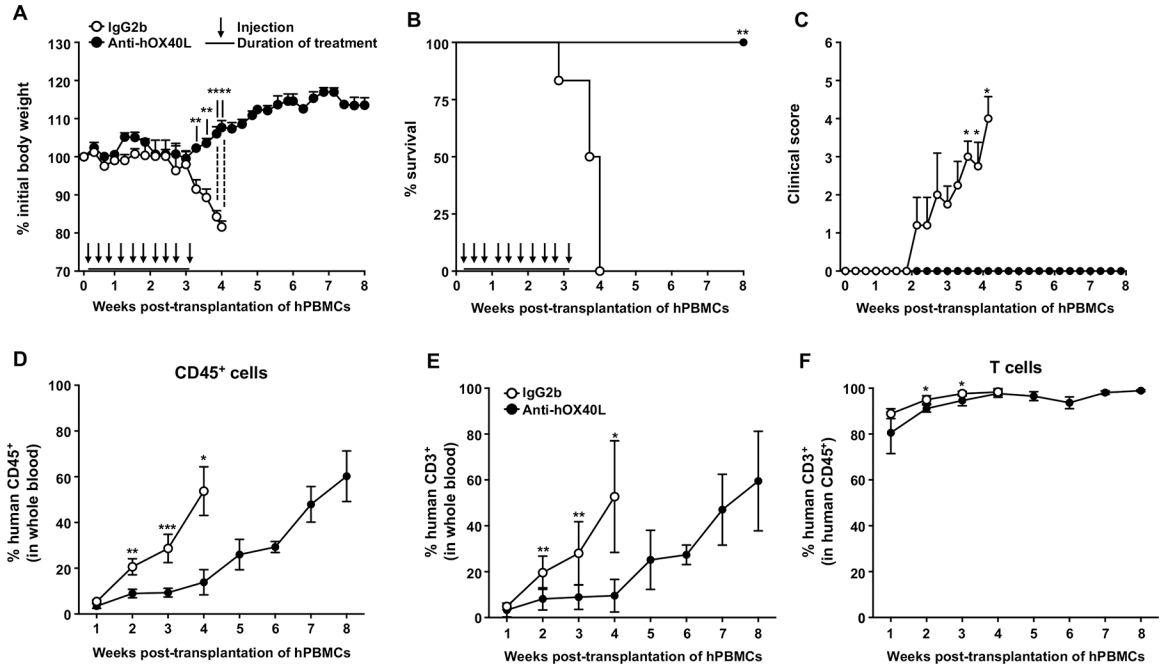

Figure 2. Anti-hOX40L treatment prevents aGVHD development in NOG mice transplanated with human peripheral blood mononuclear cells (PBMCs).

NOG mice received human PBMCs (1×10^7) via tail vein. animals were given anti-hOX40L or IgG2b (10 μg per dose) intraperitoneally 3 times weekly from day 1 post-transplantation through week 3. **(A)** Body weight changes, **(B)** Survival rates, **(C)** GVHD scores, **(D)** Frequency of circulating human $CD45^+$ leukocytes, **(E)** Frequency of $CD3^+$ T cells in whole blood, and **(F)** Frequency of human $CD3^+$ T cells in human $CD45^+$ cells. Error bars represent mean ± SD (n = 5 mice per group). Data are representative of three independent experiments. *P* values were determined with unpaired Student's *t* test in **(A, C–F)** and Mantel-Cox log-rank test in **(B)**. $*P < 0.05$, $**P < 0.01$, $***P < 0.005$.

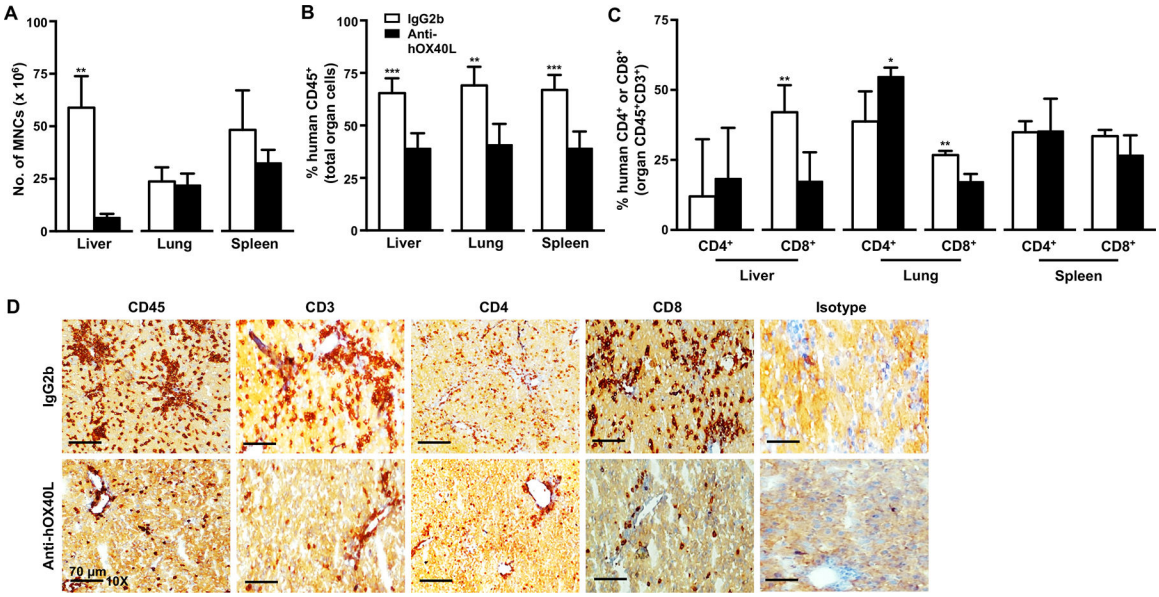

Figure 3. Anti-hOX40L treatment decreases the frequency of human T cells in livers, lungs, and spleens of aGVHD mice.

NOG mice received human PBMCs (1×10^7) via tail vein. Mice were given anti-hOX40L or IgG2b (10 µg per dose) intraperitoneally 3 times weekly from day 1 post-transplantation through week 3. Animals were sacrificed on week 4. **(A)** Total number of mononuclear cells (MNCs), **(B)** Percentage of human $CD45^+$ cells in total cells, and **(C)** Percentage of $CD4^+$ and $CD8^+$ T cells in total $CD3^+CD45^+$ T cells in liver, lung, and spleen. Error bars represent mean ± SD (n = 5 mice per group). Data are representative of three independent experiments. *P* values were determined with unpaired Student's *t* test. $*P < 0.05$, $**P < 0.01$, $***P < 0.005$. **(D)** Immunohistochemistry images (10X) of human T cell infiltration in mouse liver. Representative data from three independent experiments (n = 5 mice per group) are shown.

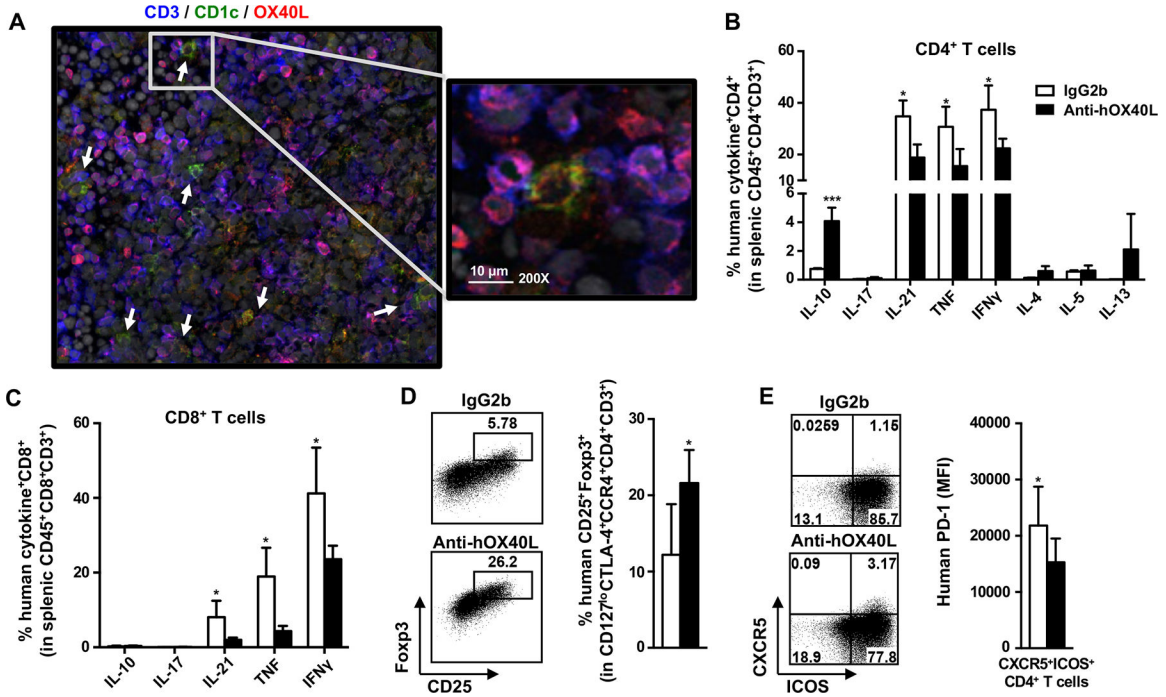

Figure. 4. Anti-hOX40L treatment reduces inflammatory T cell responses, while promoting regulatory T cell responses.

(A) Immunofluorescence of spleen. 2 weeks after human cell transplantation, spleens of an untreated x-aGVHD mice were collected and frozen sections were stained for aCD1c (green), aOX40L (red), aCD3 (blue). The outlined area on the left corresponds to the enlargement on the right. Original magnification, 20 (left) or 200 (right). Representative data are presented (n = 5 mice per group of three independent experiments). **(B - E)** Human T cells were isolated from spleens of mice received 10 dose of anti-hOX40L or IgG2b (4 weeks post-transplantation). Cells were further stained for cell surface molecules and intracellular cytokines. **(B)** Intracellular cytokine expression of $CD4^+$ **(C)** $CD8^+$ T cells after restimulated with PMA/ionomycin. **(D)** Frequency of regulatory T cells (Tregs) and **(E)** Mean fluorescence intensity (MFI) value of PD-1 expression by splenic $CXCR5^+ICOS^+CD4^+$ T cells. Error bars represent mean ± SD (n = 5 mice per group). Data are representative of three independent experiments. *P* values were determined with unpaired Student's *t* test. $*P < 0.05$, $***P < 0.005$.

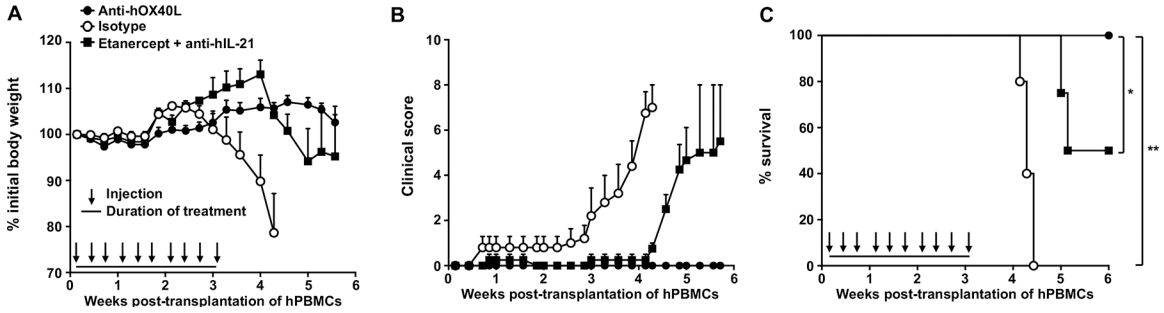

Figure 5. Anti-hOX40L is more effective than combination of etanercept and anti-hIL-21 in preventing aGVHD development.

NOG mice received human PBMCs (1×10^7) via tail vein. Mice were given anti-hOX40L (10 μg per dose), combination of anti-hIL-21 (100 μg per dose) and etanercept (100 μg per dose), or isotype (200 μg per dose), intraperitoneally 3 times weekly from day 1 post-transplantation through week 3. **(A)** Body weight changes, **(B)** clinical scores, and **(C)** survival rates were assessed. Error bars represent mean ± SD (n = 5 mice per group) and data are representative of three independent experiments. Individual *P* values were determined with Mantel-Cox log-rank test. $*P < 0.05$; $**P < 0.01$.

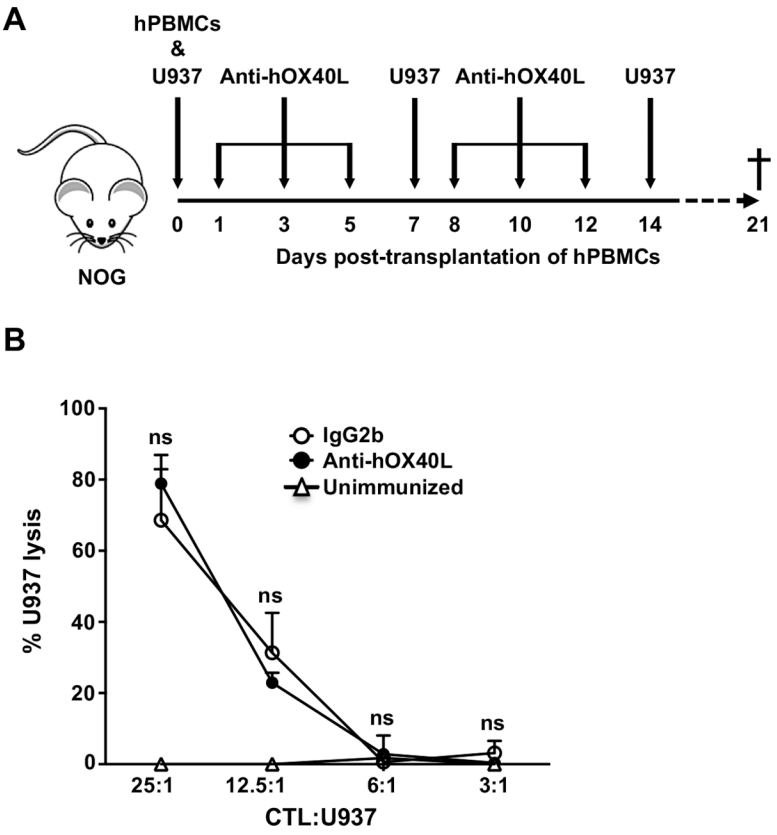

Figure 6. Anti-hOX40L treatment does not impair CD8$^+$ T cell functions.

(A) Schematic representation of experimental design. **(B)** Human CD8$^+$ T cells were purified from mouse spleens. % specific lysis was assessed by measuring fluorescence intensity after 4h incubation of CD8$^+$ T cells and U937 cells labeled with fluorochrome. Error bars represent mean ± SD (n = 5 mice per group) and data are representative of three independent experiments. Statistical significance was determined with Sidak's two-way ANOVA test. ns, not significant.

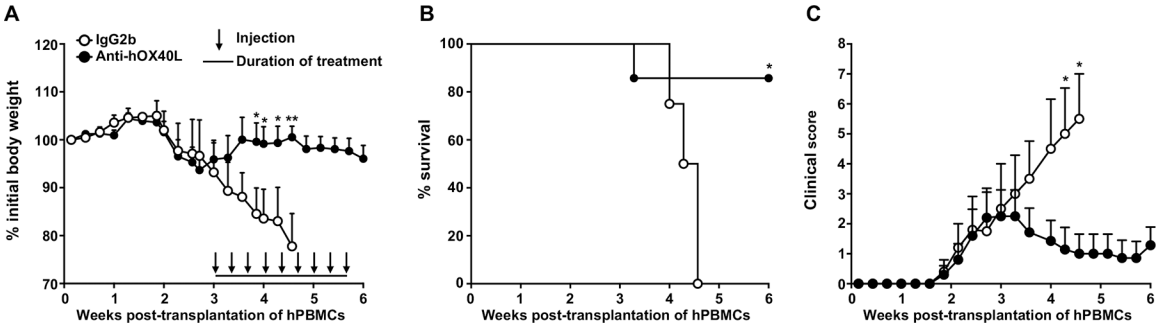

Figure 7. Preclinical therapeutic efficacy of anti-hOX40L antibody.

NOG mice received human PBMCs (1×10^7) via tail vein. animals were given anti-hOX40L or IgG2b (10 μg per dose) intraperitoneally 3 times weekly from day 21 post-transplantation through week 6. **(A)** Body weight changes, **(B)** Survival rates, and **(C)** Clinical scores were assessed. Error bars represent mean ± SD (n = 10 mice per group). Data are representative of three independent experiments. Individual *P* values were determined with unpaired Student's *t* test in **(A, C)** and Mantel-Cox log-rank test in **(B)**. $*P < 0.05$, $**P < 0.01$.